HHS Public Access

Author manuscript

Sci Signal. Author manuscript; available in PMC 2020 June 04.

Published in final edited form as:

Sci Signal. ; 12(607): . doi:10.1126/scisignal.aav4717.

Amino acid starvation enhances vaccine efficacy by augmenting neutralizing antibody production

Sumbul Afroz[1], **Shama**[1], **Srikanth Battu**[1], **Shaikh Matin**[1], **Sabrina Solouki**[2], **Jessica P. Elmore**[2], **Gillipsie Minhas**[1], **Weishan Huang**[2,3], **Avery August**[2], **Nooruddin Khan**[1,*]

[1]School of Life-Sciences, Department of Biotechnology and Bioinformatics, University of Hyderabad, Hyderabad-500046, Telangana, India

[2]Department of Microbiology & Immunology, College of Veterinary Medicine, Cornell University, Ithaca, NY, USA

[3]Department of Pathobiological Sciences, School of Veterinary Medicine, Louisiana State University, Baton Rouge, LA, USA

Abstract

Specific reduction in the intake of proteins or amino acids (AAs) offers enormous health benefits, including increased lifespan, protection against age-associated disorders, and improved metabolic fitness and immunity. Cells respond to conditions of AA-starvation by activating the amino acid starvation response (AAR). Here, we showed that mimicking AAR with halofuginone (HF) enhanced the magnitude and affinity of neutralizing, antigen-specific antibody responses in mice immunized with dengue virus envelope domain-III protein (DENVrEDIII), a potent vaccine candidate against DENV. HF enhanced the formation of germinal centers (GCs) and increased the production of the cytokine IL-10 in the secondary lymphoid organs of vaccinated mice. Furthermore, HF promoted the transcription of genes associated with memory B cell formation and maintenance and maturation of GCs in the draining lymph nodes of vaccinated mice. The increased abundance of IL-10 in HF-preconditioned mice correlated with enhanced GC responses and may promote the establishment of long-lived plasma cells that secrete antigen-specific, high-affinity antibodies. Thus, these data suggest that mimetics of AA-starvation could provide an alternative strategy to augment the efficacy of vaccines against dengue and other infectious diseases.

*Corresponding author. noor@uohyd.ac.in.

Author contributions: NK conceptualized the study. SA designed and performed most of the experiments with assistance from SB. S. and SM expressed and purified the recombinant DENVrEDIII protein. SS, JE and WH performed experiments in WT and *Gcn2*$^{-/-}$ C57Bl/6 mice. NK, SA, SB and AA wrote the manuscript. SB made the figures. SA, AA and NK interpreted the data. GM assisted during experiments.

Competing Interests: AA receives research funding from 3M Corporation. All other authors declare that they have no competing interests.

Data and materials availability: All data needed to evaluate the conclusions in the paper are present in the paper or in the Supplementary Materials.

Introduction

Metabolic regulation of the immune system is evolutionarily conserved and paramount for overall organismal health (1, 2). Nutrient uptake and nutritional status affect immune cell proliferation, differentiation and survival (3). In this regard, epidemiological and clinical studies indicate that malnutrition impairs host immune responses and increases rates of morbidity and mortality after infection (4, 5). Similarly, reduced intake of nutrients without malnutrition, often termed as Caloric or Dietary Restriction (CR or DR), improves metabolic fitness and longevity (6) and provides enormous benefits against age-associated disorders such as neurological, cardiovascular and skeletal problems (7, 8). Exceptions include prolonged energy restriction in small animals, which can reduce growth and development of lymphoid organs and impair antigen specific immune responses(9, 10). The benefits of CR during viral infections are largely dependent on body weight and may vary between different animals (11–14). Small and aged animals subjected to long-term CR are more susceptible to Influenza infection, due to continuous body mass loss and accompanying energy deficits that impair recovery, despite increased splenocytes proliferation(11). However, short-term re-feeding after energy restriction in mice restores body weight and fat composition, as well as Natural Killer cell function required to combat Influenza infection (13). Emerging evidence suggests that CR has a beneficial impact on various attributes of the immune system. These include enhancing thymopoiesis and maintainence of T-cell diversity (15), natural killer and $CD4^+$ and $CD8^+$ T-cell activity(16–18), and the apoptotic clearance of senescent T-cells in aged mice (17, 19, 20). Furthermore, CR stimulates adaptive immunity against parasitic infection in experimental cerebral malaria (21).

Although the associated benefits of CR are mostly linked to reduced calorie intake, accumulating evidence couples dietary amino acid (AA) restriction to the benefits of CR (8). For instance, AA sensing pathways influence both innate and adaptive immunity (22). Innate immune cells are auxotrophs for AAs and sense the availability of extracellular AAs through their intrinsic metabolic sensing pathway (8, 23). AA-depletion results in the accumulation of uncharged tRNAs, which are sensed by general control nonderepressible-2 kinase (GCN2) (24) and trigger its activation. Activated GCN2 phosphorylates eukaryotic translation initiation factor 2α (eIF2α), which results in the activation of amino acid starvation response pathway (AAR) that coordinates post-transcriptional and translational immune reprogramming (25, 26). The AAR can also be activated by Halofuginone (HF), a derivative of the Chinese herb *Dichroa febrifuga*, which creates a pool of uncharged tRNA by inhibiting prolyl-tRNA synthetase(26), mimicking the effects of AA-starvation (27). Indeed, HF has garnered substantial attention in the last two decades owing to its therapeutic potential in various diseases including autoimmune disease, cancer, muscular dystrophy, hepatic and renal ischemia-reperfusion injury (26, 28–32).

Activation of the AAR using HF or amino acid restricted diet abrogates the production of IL-1β through the GCN2 pathway, and provides protection against intestinal inflammation in an experimental mouse model (25, 33). Furthermore, HF inhibits T_H17 cell differentiation and provides protection against experimental autoimmune encephalomyelitis (34). In addition, a molecular signature comprising of GCN2 correlates with the $CD8^+$ T-cell response to the Yellow Fever Vaccine-17D (YF-17D)(35, 36). Furthermore, the GCN2

pathway is crucial for optimal proliferation in response to antigen stimulation in vitro, and for the appropriate trafficking of $CD8^+$ T-cells to lymphoid organs (37). These findings raise the intriguing possibility that the activation of the AAR pathway with HF could enhance the immunogenicity of vaccine antigens.

While rates of dengue virus (DENV) infection are increasing, there is still no licensed vaccine to date that is effective against all DENV serotypes(38). Therefore there is an urgent need to identify strategies that can enhance the neutralizing antibody response to all the four serotypes of DENV and promote long term vaccine protection. We used the recombinant envelope protein domain III (EDIII) of DENV as a model vaccine antigen in our study, because it is considered as one of the most potent vaccine candidates against DENV(39). Our results demonstrated that HF increased numbers of DENV EDIII-specific IFN-γ and IL-2 producing $CD4^+$ and $CD8^+$ T cells in mice. HF also increased the amount and affinity of DENV EDIII-specific IgG in the serum of vaccinated mice and its neutralizing activity against all the four serotypes of DENVs. These changes were accompanied by enhanced production of IL-10 and expression of gene signatures involved in antigen-specific memory B-cell formation, proliferation and differentiation of GC B-cells in the draining lymph nodes of vaccinated mice. Collectively, these findings highlight a promising role for HF in enhancing robust antigen-specific immunity against vaccine antigens, and further suggest a potential application of manipulating AAR through AA restriction mimicry for the design and development of new vaccines.

Results

AA-starvation mimetic HF enhances antigen-specific T-cell responses

The amino acid starvation sensor, GCN2 promotes the development of protective immune responses triggered by YF17D vaccine (36). To evaluate the effect of AA-restriction on antigen specific T-cell immunity, we used HF, a pharmacological activator of AAR, and DENVEDIII antigen, a potential vaccine candidate against DENV. We first purified 6X-His tagged recombinant EDIII of all the four DENV serotypes, with the purity and molecular weights verified on Coomassie-stained SDS-PAGE gel, and specificity of the proteins confirmed by immunoblotting (fig. S1A, B). The purified proteins were Polymixin bead treated to remove any endotoxin content prior to use in immunization studies. DENV-2 EDIII (DENVrEDIII) was administered in mice pre-conditioned with HF or DMSO control (Fig. 1A). Because HF activation of the AAR pathway induces eIF2-α phosphorylation, which promotes cellular translational arrest and ATF4 transcription factor expression(34, 40), we evaluated eIF2-α phosphorylation and the expression of ATF4 target genes including *eIF4Ebp1, Chop, Asns* and *Gpt2* in the splenocytes of immunized mice. We found that HF treatment increased phosphorylation of eIF2-α and activation of ATF4 target genes (fig. S2A, B). Further, HF treatment promoted eIF2-α phosphorylation in immune cells including B-cells, T-cells and dendritic cells (fig. S2C and D) when administered in mice, with no changes in the body weight of HF-treated mice (fig. S2E). Next, we examined the effect of AAR activation on the magnitude of DENVrEDIII specific T-cell responses following primary immunization. We found that HF treatment enhanced ^{3}H-thymidine incorporation by DENVrEDIII re-stimulated splenocytes from immunized mice, suggesting

that HF increased the expansion of antigen-specific lymphocytes (Fig. 1B). We also found that HF-treatment enhanced DENVrEDIII induced production of IFN-γ by DENVrEDIII restimulated $CD8^+$ and $CD4^+$ T-cells from blood, spleens and lymph nodes at 4 weeks post-secondary immunization (Fig. 1, C to J). Similar results were observed for the production of antigen-specific IL-2 (fig. S3A–D). The $CD8^+$ and $CD4^+$ T-cell responses in PBMCs were more rapid and robust when HF or DMSO preconditioned mice were immunized with DENVrEDIII protein (Fig. 2A). Although there is a reduction in T-cell responses after 4 weeks, the enhanced DENVrEDIII specific induction of IFN-γ secreting T-cells was nevertheless evident in the HF-treated group (Fig. 2A). The reduction in effector $CD8^+$ and $CD4^+$ T cell responses with time occurs during the contraction phase, allowing the maintenance of T-cell homeostasis and avoiding non-specific immunopathology that may be generated due to large number of activated T-cells in the host (41, 42). Polyfunctional T cells, which are largely memory T-cells, secrete multiple cytokines including IFN-γ, IL-2 and TNF-α, and are associated with providing increased protection against the pathogens (41, 43). Our results indicate that HF treatment increased the frequency of antigen-specific polyfunctional double cytokine producing (IFN-γ, IL-2) $CD8^+$ and $CD4^+$ T cells found in immunized mice after DENVrEDIII restimulation (Fig. 2, B and C). This increase was most notable in the DENVrEDIII reactive polyfunctional T cell (IFN-γ^+IL-2^+) subsets (Fig. 2D). Further, splenocytes and lymph node cells from HF pre-treated mice showed increased production of IFN-γ, IL-12p40 and TNF upon DENVrEDIII stimulation (Fig. 3). Secretion of these pro-inflammatory cytokines provide a third signal for effector T cell expansion (44) and indicate enhanced antigen-specific cellular response under the conditions of AAR activation. Altogether, these results point towards a role for AAR activation in enhancing the magnitude and quality of antigen-specific $CD4^+$ and $CD8^+$ T cell responses, perhaps in part by augmenting the delivery of antigen to antigen presenting cells (APCs) as previously reported (36).

HF enhances antibody responses against DENV envelope domain III (DENVrEDIII) protein

The activation of $CD4^+$ T-helper cells is a vital step in establishing an adaptive immune response, acting both as an effector and a modulator of the immune response. $CD4^+$ T helper cell differentiation into T follicular cells (Tfh) provides a vital signal that drives the activation and differentiation of high-affinity memory B cells and antibody-producing plasma cells (45, 46). Having observed the effect of HF on induction of robust antigen-specific $CD4^+$ T cell responses, we further determined the effects of HF on antigen-specific antibody responses. We assessed the amount of DENV-2 EDIII specific total IgG and IgG subtypes IgG2a, IgG2b and IgG1 in the serum from DENVrEDIII immunized mice preconditioned with HF or vehicle control following both primary and secondary immunization. We observed a significant increase (more than 2-fold) in the production of DENVrEDIII-specific total IgG and in all the IgG subtypes in the serum of HF preconditioned mice (Fig. 4A). Secondary immunization with the same immunogen two weeks later, enhanced antibody amounts in all immunized groups, and again significant enhancement was evident in DENVrEDIII+HF immunized group (Fig. 4A). The production of Ovalbumin (OVA) specific antibodies (total IgG and IgG subtypes) was also enhanced when HF primed mice were immunized with OVA antigen as compared to vehicle control

DMSO (fig. S4). These results establish that activation of the AAR pathway may enhance antigen-specific immune responses for diverse antigens.

To determine whether HF enhances antigen-specific responses through GCN2, we evaluated the amount of DENVrEDIII specific antibodies in the serum of HF or DMSO preconditioned WT or *Gcn2*$^{-/-}$ mice immunized with DENVrEDIII protein. We found that HF had no effect on antigen-specific total IgG or IgG subtypes responses in *Gcn2*$^{-/-}$ mice, while we observed a significant increase in antibody responses in HF pre-conditioned WT littermate controls (fig. S5). This data supports the conclusion that HF enhances antigen-specific immune responses through GCN2, and not through off-target effects.

HF augments the quality of antigen specific antibody responses

T-cell dependent B-cell activation is predominantly characterized by the development of high affinity antibodies mostly the IgG subtype(45), and the avidity of antigen-antibody interaction is one of the parameters that determines the quality of the antibody responses(47). We examined the binding response and avidity of DENV-2 EDIII (DENVrEDIII) specific antibodies using surface plasmon resonance (SPR) assay. Serum samples taken from mice 28 days after the secondary immunization, were assayed for binding to immobilized DENVrEDIII on CM5 sensor surface. With DENVrEDIII secondary immunization, serum from HF pre-treated mice gave the highest antigen binding response (in RU) as compared to vehicle control pre-treated mice (Fig. 4B). SPR analysis of two-fold serial dilution of the serum (ranging from 1:50 to 1:400) from HF-preconditioned immunized mice indicated stable association with DENVrEDIII compared to the sera from unimmunized or DMSO-preconditioned control mice (fig. S6). The qualitative analysis of the DENVrEDIII specific antibody response was evaluated in terms of avidity by measuring the dissociation rate constants. Serum from HF-preconditioned, DENVrEDIII-immunized mice associated with DENVrEDIII protein faster and dissociated from DENVrEDIII slower, suggesting that HF-induced enhanced high–affinity antibody responses (Fig. 4C). Increased amounts of antigen specific, high-avidity antibody after DENVrEDIII vaccination with HF pre-treatment correlated with improved antibody function as assessed by the virus neutralizing ability in vitro. Serum from mice immunized with DENVrEDIII after HF preconditioning neutralized DENV-2 virus more efficiently than serum from mice immunized with DENVrEDIII after vehicle control treatment (Fig. 4D). We also observed a significant increase in DENV serotype specific total serum IgG when we immunized HF preconditioned mice with a tetravalent formulation consisting of domain III proteins of all the four DENV serotypes (tDENVrEDIII) (Fig. 5A). In addition, the resultant antibodies were effective against DENV-1, 2, 3 and 4 serotypes (Fig. 5B). Altogether, the above results indicate that activation of the AAR pathway enhances both the magnitude and quality of antigen-specific B-cell responses.

HF induces enhanced development of germinal centers in draining lymph nodes

GCs are crucial for humoral immunity and play a vital role in the development of immunological memory. The explicit co-localization of antigen-specific T-cells, B-cells and follicular dendritic cells (FDCs) is crucial for GC formation (48). The progression of B cell responses along the GC pathway is important in the generation of long lived-plasma cells

that secrete high affinity antibodies (49). Since our results suggest that HF enhances the production of high avidity antibodies, we determined whether activation of the AAR axis regulates the GC pathway. Thus, immunized mice preconditioned with HF or DMSO were sacrificed on day 28 after the booster dose, inguinal lymph nodes were isolated, and the presence of GCs was evaluated by immunohistology. We found that HF preconditioned, DENVrEDIII immunized mice developed more lymph node GCs than DMSO preconditioned, DENVrEDIII immunized mice (Fig. 6A, B), which were also apparent in haematoxylin and eosin (H&E) stained sections of inguinal lymph nodes (fig. S7A, B). To determine the persistence of GC responses in HF preconditioned mice, we examined GC kinetics over a duration of eight weeks by evaluating the frequency of GC B-cells in the draining lymph nodes using flow-cytometry (fig. S7C). We observed a significant increase in GC expansion within 10 days of antigen immunization, with increased frequency of $B220^{+}GL\text{-}7^{+}IgG^{+}$ GC B-cells in the lymph nodes of DENVrEDIII immunized mice primed with HF (Fig. 6C). The GC responses peaked at 28 days after antigen boost, correlated with the antigen specific antibody responses, followed by a decline. The decline in GC responses at later time-point is perhaps a result of reduction in the number of $CD4^{+}$/Tfh cells, which is a prerequisite for establishing optimal GC reactions for effective protective immunity, while avoiding the production of low affinity self-reactive antibodies that lead to autoimmunity(50, 51).

The pleiotropic cytokine IL-10 has a key role in the generation of GC B-cell responses. IL-10 produced by $CD4^{+}$ follicular T-cells (52) and B-cell intrinsic IL-10 signalling(53) have been observed to directly promote GC responses. Therefore, we measured the amount of IL-10 in the DENVrEDIII restimulated splenocytes and lymph node cells from the immunized mice, and found elevated IL-10 production from cells of HF-preconditioned mice (Fig. 6D), highlighting an important role for IL-10 in AAR mediated regulation of GC responses. We speculated that the effects of AAR activation on the germinal centre pathway might be due to transcriptional programming of genes in antigen-specific B-cells, thus we carried out qRT-PCR analysis to look for the molecular signatures involved in the maintenance of GCs in draining lymph nodes. We observed enhanced expression of genes associated with programming of memory B-cells in the lymph nodes of HF preconditioned DENVrEDIII immunized mice. Memory B-cells swiftly respond to booster immunization thereby driving the localization of antigen-specific plasma cells to surviving niches in bone marrow, generating long-lived plasma cells that are the primary source of high avidity antibodies in serum(54). Notably HF-preconditioning induced AAR activation enhanced the expression of genes involved in maintaining the integrity of GCs (*Bcl2*(55), *Tank*(43)), genes crucial in formation and maintenance of B-cell memory (*Plcg2*(56), *Cd38*(57)),genes involved in the proliferation, survival and differentiation of GC B-cells such as (*Il17ra*(58), *Il18r1*, *Pax5*(59), *Ikzf1*(60)) and *Irf7* and *Mx1*, type-1 interferon genes involved in differentiation of B-cells (Fig. 6E). These findings exemplify the benefits of AA restriction in the production of robust high avidity and neutralizing antibody mediated through programming of genes associated with memory B cell development and differentiation. Hence, this study suggests that AAR pathway might be manipulated for the design and development of vaccines for tailoring long-lived protective immunity against the pathogens.

Discussion

Metabolic control of the immune system is a crucial requirement for the regulation of cell survival, and the development of immunity (1). Accumulating evidence suggest that the immune system can sense and respond to diverse changing environmental signals, including fluctuations in the abundance of amino acids and other metabolites. Metabolic sensors like GCN2 are able to sense depletion of even a single type of amino acid in the cellular microenvironment and respond appropriately through the activation of AAR pathway, which in turn can dictate and tailor the fate of immune cells (61). Although activation of the GCN2-AAR pathway has broad anti-inflammatory effects (25, 33) and therapeutically benefits various metabolic diseases (26), the impact of AAR on the adaptive immune response in infectious disease remains poorly characterized. GCN2 stimulates protective immunity to YF17D, one of the most successful vaccines developed (36). In the present study, we have used a plant derived biomolecule, HF, to activate the AAR pathway (34) and evaluated its role in tailoring the protective efficacy of vaccines in a mouse model using DENV envelope protein domain III (DENVrEDIII) as a model antigen. Our results highlight a critical role of AAR pathway in the regulation of T and B cell immunity to DENVrEDIII antigen.

HF enhanced T-cell responses, including the frequency of IFN-γ, and IL-2, and double cytokine (IFN-γ and IL-2) producing $CD8^+$ and $CD4^+$ effector and polyfunctional T-cells. The latter are a prerequisite for antigen-specific protective T-cell adaptive immunity(41, 43). Furthermore, the DENVrEDIII specific T-cell recall responses correlated with the magnitude of antigen specific antibody responses after AAR activation. Effective vaccines establish protective humoral immunity, which depends on the production of long-lived plasma cells secreting high affinity antibodies that are necessary for pathogen clearance(62). The activation of the AAR pathway enhanced production of high avidity and greater virus neutralizing antibody titres, which were able to efficiently neutralize all the serotypes of dengue virus, one of the key goals of DENV vaccine development. T cell activation promotes neutralizing antibody production by stimulating the development of GC in response of antigenic challenge (63), and our results demonstrate that AAR activation enhanced the formation of GCs in the draining lymph nodes of HF pre-treated mice. HF pre-conditioning also promoted production of the cytokine IL-10, which is involved in GC formation (53). Our data suggest that AAR activation might increase the establishment of GCs through enhanced IL-10 production, and thereby improve antigen-specific humoral immunity. Supporting the antigen driven nature of this response, we did not observe GC formation in the lymph nodes from mice 5 days post HF pre-conditioning only, demonstrating that the GC phenotype did not exist prior to antigen immunization, or that HF priming merely resulted in the production of self-reactive antibodies.

Our results suggest that AAR activation stimulates a molecular program that aids in the differentiation, maintenance and survival of GC B-cells, thereby augmenting immunological memory. For example, B-cell lymphoma 2 (*Bcl2*) is involved in maintaining the integrity of GC by inhibiting apoptosis within the GC B-cells(55). The *Plcg2* gene product conveys survival signals to GC and memory B-cells necessary for the generation of the secondary immune responses(56). Additionally, signalling through IL-17RAis required to secure the

localization of Tfh cells in the GC to induce its function, stabilizing the interaction of GC-B-cells with nearby T-helper cells(58). Pax5 (Paired box protein 5) is a master regulator of B-cell development and is expressed in pro-B cells to mature GC B-cells(59). Pax5 works in coordination with other proteins critical for B-cell function, and drives the expression of Interferon regulatory factors such as IRF8, thereby contributing towards sensing the advancement of GC reaction(59, 64). Our data demonstrated that HF treatment augmented the expression of all of these critical B cell survival factors.

Taken together, these data demonstrate that HF augmented GC formation, which enhanced the magnitude and quality of antigen-specific antibody responses and correlated with transcriptional reprogramming of lymphoid organs, after experimental DENV vaccination. Although this work demonstrates the feasibility of using HF to enhance vaccine responses, the mechanisms by which AAR promotes germinal centre formation remains poorly understood and merits further investigation. Further, the detailed study of the T-cell dependence of the effects of HF on antigen specific antibody responses could be the next step. However, our data demonstrate that AAR mimicry based nutraceuticals such as HF are potent agonists of vaccine responses poised for further development against human diseases.

Materials and Methods

Purification of recombinant DENV envelope domain III protein (DENVrEDIII)

The optimized envelope domain III sequence for all the four DENV serotypes (DENV-1, 2, 3 and 4) were cloned into bacterial expression vector pET-28a by Genescript (USA). The cloned constructs were expressed in *E. coli* strain Rossetta and induced with 0.6mM IPTG (DENV-2) or 1mM IPTG (DENV-1, 3 and 4). The 6X His tag recombinant Dengue envelope protein domain III (DENVrEDIII) was purified using affinity chromatography technique under denaturing conditions as described earlier(65)using Talon Superflow (GE Healthcare) high affinity resins. The His-DENVrEDIII proteins were eluted using 300 mM Imidazole, run on SDS-PAGE and subjected to Coomassie staining. The desired band size of 14.5 kD (DENV-1, 2 and 4) and 15 kD (DENV-3) was observed in the Coomassie stained gel.

Immunoblotting

The 6X His tagged purified Dengue envelope domain III (DENVrEDIII) protein for all the four serotypes was confirmed by immunoblotting using anti-His antibody (Cell Signalling). For evaluation of Halofuginone (HF) mediated AAR activation, splenocytes from immunized mice were lysed in lysis buffer (1% Triton-X 100, 150 mM NaCl, 1 mM EDTA, 10% Glycerol, 20 mM HEPES, pH 7.5, 100 mM NaF, 17.5 mM β-glycerophosphate and supplemented with 1X Protease Inhibitor Cocktail (Sigma Aldrich))(25), incubated on ice for 30 min. and cleared by centrifugation at 12000 rpm for 15 min. at 4°C. Equal amount of protein were separated on SDS-PAGE and transferred to nitrocellulose membrane. For the detection of eIF2α phosphorylation, the membrane was blocked with 5% bovine serum albumin and probed with rabbit anti-eIF2α-P antibody (Cell Signalling). Protein bands were visualized with FemtoPlus ECL chemiluminescent substrate. Densitometry analysis of eIF2α-P bands with respect to eIF2α-T bands was done using NIH software Image J.

Immunization of mice

Six to eight week old Balb/c mice were administered intraperitonially (i.p.) with 0.1mg/kg body weight (bw) Halofuginone (HF) or vehicle control (DMSO)(34) for four days followed by immunization with 20μg/mouse per dose of DENV-2 envelope domain-III protein (DENVrEDIII) in 200μl 1XPBS, delivered subcutaneously (s.c.) at the base of the tail, followed by resting for ten days. The booster injection was given at the 14^{th} day post primary immunization with an identical dose of HF or DMSO (i.p.) again for four days, followed by s.c. administration of 20μg/mouse per dose DENVrEDIII protein. The mice were rested for ten days, and euthanized at the 28^{th} day after primary injection for further analysis of blood, spleen and lymph node cells. In another set of experiments, Balb/c mice previously conditioned with HF or DMSO were immunized by s.c. injection of tetravalent DENV envelope domain III protein (tDENVrEDIII) formulation (10μg each of DENV-1, 2, 3 & 4 rEDIII) following the same regimen as mentioned above. In yet another experiment Balb/c mice previously conditioned with HF or DMSO were injected subcutaneously with 10μg of Ovalbumin (Ova) as antigen/mouse per dose following the same immunization schedule as mentioned above. Blood samples were collected on the 14^{th} and 28^{th} day by tail bleeding for serum collection and PBMC isolation. In another set of experiments WT or *Gcn2*$^{-/-}$ mice (on a C57Bl/6 background) were immunized with 20μg DENVrEDIII antigen/mouse post HF or DMSO priming following the above mentioned immunization schedule. Blood samples were collected at the 14^{th} and 28^{th} days by tail bleeding for serum collection for the analysis of antigen-specific antibody responses. Animals that were injected with PBS alone (without candidate antigen) served as negative controls. All animal experiments were performed according to the animal ethical guidelines of the University of Hyderabad and the Institutional Animal Care and Use Committee at Cornell University.

Phospho-eIF2α staining by flow cytometry

Total splenocytes isolated from HF or DMSO pre-conditioned mice were surface stained using PerCP Cy5.5 anti-mouse CD45R/B220 (BD Pharmingen), APC anti-mouse CD11c (BD Pharmingen), and Alexa-Fluor 700 anti-mouse CD3 (eBioscience) at 4°C for 30 min. The stained cells were washed with FACS buffer and quickly fixed using 4% paraformaldehyde followed by intracellular staining for eIF2α-P as described earlier (33). Fixed cells were permeabilized using 1X Perm Wash Buffer (Bio Legend) and incubated with rabbit anti-mouse monoclonal eIF2α-P antibody (Cell Signalling) or respective isotype control overnight at 4°C. Following washes with 1X FACS buffer, the cells were stained with anti-mouse Alexa488 secondary antibody for 1h at room temperature, washed and re-suspended in FACS buffer and acquired on BD LSR Fortessa (BD Biosciences) cytometer and analyzed using FlowJo (Tree Star Inc).

T-cell assays by flow cytometry

Lymph node and spleen $CD4^+$ and $CD8^+$ T-cells from immunized mice (collected at day 28), and those from peripheral blood mononuclear cells (PBMCs) (collected at day 14 and day 28), were evaluated for antigen specific responses. PBMCs were isolated by sucrose gradient density separation method using Histopaque (Sigma Aldrich) as described earlier(66). Briefly, isolated PBMCs, lymph node cells and splenocytes were cultured for restimulation

with 10μg ml^{-1} DENVrEDIII protein in the presence of Golgi Stop and Golgi Plug (BD Biosciences) at 37°C for 10 hrs. The restimulated cells were stained with Alexa-488 labelled anti-mouse CD8 (BD Biosciences) and PerCP (eBiosciences) or FITC labelled anti-mouse CD4 antibodies (BD biosciences) for 60 min. at 4°C. The cells were further washed 3X with FACS buffer, fixed with 4% paraformaldehyde, permeabilized using 1X Perm Wash Buffer (Bio legend), and stained using APC labelled anti-mouse IFN-γ (BD Biosciences) and PE conjugated anti-mouse IL-2 antibody (BD Biosciences), diluted in 1X Perm Wash Buffer for 60 min. at room temperature. Cells were washed with FACS buffer and data acquired on BD LSR Fortessa (BD Biosciences) cytometer and analyzed using FlowJo (Tree Star Inc).

Cytokine secretion by ELISA and proliferation assay

The cytokines secreted were evaluated in splenocytes and lymph node cells isolated from immunized mice. 2×10^5 splenocytes or lymph node cells were seeded in triplicates in 96-well round bottom plate and restimulated with 10μgml^{-1} DENVrEDIII for 72h. The supernatants were then collected and analyzed for IFN-γ, IL-12p40, TNF-α and IL-10 (BD Biosciences) cytokines through sandwich ELISA following the protocol as per manufacturer's instructions. Lymphocyte proliferation was assessed in 72h splenocytes culture as mentioned earlier(67). Briefly, after 72h, splenocytes were pulsed with 1 μCi [^{3}H] thymidine for additional 16h. Cells were harvested, fixed with 10% TCA for 30 min. at room temperature followed by solubilization with 150 μl of 1N NaOH for 30 min. at 37°C with constant agitation. Next, 150 μl of 1N HCl was immediately added; 300 μl of each sample was mixed with 5ml of scintillation fluid (Sisco Research Laboratories) and the counts were measured in a scintillation counter (PerkinElmer).

Antibody ELISA

For detection of antigen specific antibodies in the serum of immunized mice, 100μl of 5 μg ml^{-1} of DENVrEDIII proteins diluted in Carbonate Buffer were coated on 96-well Nunc Maxisorp ELISA plates and incubated overnight at 4°C. Next, the plates were washed 3X with 1X PBST (0.05%Tween 20) using a Thermo Fisher Scientific Well wash 4 MK 2 ELISA washer. The plates were blocked using 4% skimmed milk (Hi Media) for 1hr at room temperature. Serum samples were diluted in 0.1% skimmed milk prepared in 1XPBS and incubated on blocked plates for 2 h at room temperature. Following 5X washes with 1X PBST, the plates were incubated with anti-mouse IgG (whole molecule)-Peroxidase (1:5000, Sigma Aldrich), anti-mouse IgG2a-HRP (1:2000, Santa Cruz), anti-mouse IgG2b-HRP (1:2000, Santa Cruz) and anti-mouse IgG1-HRP (1:5000, Santa Cruz) diluted in 1X PBS for 1hr at room temperature. After washing 6X with 1X PBST, the plates were finally developed with 100 μl per well of Tetramethylbenzidine (TMB) substrate (BD Biosciences). The reaction was stopped using 2N H_2SO4. Plates were analyzed using Tecan microplate reader at λ =450nm and correction at λ =570nm(67).

BIAcore Assay

Surface Plasmon Resonance (SPR) binding and kinetics measurement were carried out at 25°C on a BIAcore T200 instrument (BIAcore/GE Healthcare) as described earlier(43, 68, 69). The CM-5 sensor chip (GE Healthcare) was immobilized with DENVrEDIII (for serotype 2) diluted in 10mM Sodium acetate, pH 4.5, using standard amine coupling

chemistry. Serum samples collected at day 28 from immunized mice were injected at 1:50 to 1:400 dilution by using two-fold dilution steps at a flow rate of 30μl min^{-1}. The contact time for the serum samples to interact with ligand immobilized on the sensor chip was 60s and dissociation time for the sample was 60s. After each cycle, the sensor chip was regenerated with 50mM NaOH with a specified contact time for 60s. The experimental data were fit using 1:1 Langmuir model for determining the binding kinetics, analysis was performed using BIAcore T200 Evaluation software version 2.0. To analyze antigen (DENVrEDIII) specific antibody binding avidity, maximal response unit (RU_{max}) and dissociation rates (k_d) were measured. Avidity scores were determined as mentioned earlier (Avidity score= Maximum Binding response/k_d in RUs)(62).

Dengue Virus stock preparation

DENV-1 (Hawaii), DENV-2 (TR1751), DENV-3 (Thailand 1973) and DENV-4 (Columbia 1982) viral strains were propagated in C636 cells as described earlier(70). Viral titres were quantitated by Focus Forming Assay in BHK-21 and Vero cells as previously described (71).

Focus reduction neutralization tests (FRNT)

FRNT was carried out in Vero cells seeded at a density of 25,000 cells in 96 well plate 24h prior to infection as described earlier(72, 73). Serum samples from immunized mice were heat activated at 56°C for 30 min. and were two fold serially diluted (from 1:12.5 to 1:3200) in serum free DMEM medium. Following de-complementation and dilution of serum, 50μl of each dilution was thoroughly mixed with 50 PFU Dengue virus (DENV-1, 2, 3 and 4) diluted in DMEM and incubated at 37°C for 2h. Next, Vero cells were washed with serum free DMEM and infected in duplicate with 45μl of the neutralization mixture followed by another incubation for the next 2h. Following incubation, the viral inoculum was removed and overlaid with 200μl of 1.5% carboxymethylcellulose (Sigma Aldrich) in serum free DMEM and incubated at 37°C for 4–5days depending upon the serotype. After incubation the overlay media was carefully removed followed by three washes with 1XPBS. The cells were further fixed, permeabilized with 0.2% Triton X-100 and stained with anti-dengue monoclonal antibody (GeneTex) for 1h at 37°C. Post washing with 1XPBS, the stained cells were incubated with HRP-linked anti-mouse secondary Ab for 1 h at 37°C. The cells were finally washed with 1XPBS and developed using DAB substrate. Viral foci were counted manually and the percentage of foci reduction against control serum calculated. Neutralizing antibody titre ($FRNT_{50}$) values were determined as the reciprocal of the highest dilution that resulted in 50% decrease in focus forming units and analyzed using Graph Pad Prism Software.

Quantitative Real time PCR (qRT-PCR)

Germinal centre gene expression profiling was done on DENVrEDIII (serotype 2) restimulated cells isolated from lymph nodes of different immunized mice. Total RNA was extracted using TRI reagent (Sigma Aldrich) as described earlier(73). Total purified RNA was reverse transcribed using Easy Script cDNA synthesis kit (abm) according to manufacturer's instructions. Quantitative real-time PCR was performed using Applied Biosystems QuantStudio5. The cDNA was amplified using Syber-Green Mix (Kappa Biosystems) with gene - specific primers (Table S1) following thermo cycler program of one

cycle of 95 °C for 10min, next 40 cycles of 15s at 95 °C, 30s annealing at 56°C and 40s extension at 68°C. The relative mRNA expression was normalized to housekeeping gene *Gapdh*. The normalized expression of statistically significant genes are presented as Heat Map using Gene-e software (www.broadinstitute.org). Genes with $P<0.05$ (two tailed unpaired student *t* test) were considered significant. Activation of AAR pathway genes were evaluated in splenocytes from immunized mice. The mRNA expression of AAR genes were determined using gene-specific primers (Table S1) and normalized to housekeeping gene *Hprt*.

Histology and Immunofluorescence

Draining lymph nodes were isolated and snap frozen in OCT tissue embedding medium for sectioning as mentioned earlier(43, 67). Sections were either stained with haematoxylin & eosin (HE) or fluorescently stained with Alexa 488 labelled anti-mouse B220 (eBiosciences), Alexa 647 labelled anti-mouse total IgG (Cell Signalling) or Biotin labelled anti-GL7 (eBiosciences) followed by Alexa 555 labelled Streptavidin (Invitrogen) antibodies. The slides were washed and mounted with cover slips using DPX mounting medium. The images were captured using a 40× objective on a Zeiss confocal microscope.

Germinal Centre staining by flow cytometry

For identification of germinal centres by flow-cytometry, cells isolated from lymph nodes collected at the 5^{th} day (post HF or DMSO priming), 14^{th}, 28^{th} (post booster), 42^{nd} and 56^{th} day were passed through 40μm cell strainer to generate single-cell suspensions following which they were stained with Alexa 488 labelled anti-mouse B220 (eBiosciences), Alexa 647 labelled anti-mouse total IgG (Cell Signalling) or biotin labelled anti-GL7 (eBiosciences) for 1h at 4°C, followed by Alexa 555 labelled Streptavidin (Invitrogen) for 1h at room temperature. The stained cells were fixed using 4% paraformaldehyde, washed with FACS buffer and data acquired on BD LSR Fortessa (BD Biosciences) cytometer and analyzed using FlowJo (Tree Star Inc).

Statistical Analysis

Statistical analysis was done using Graph Pad Prism 7 Software. Normality test (Shapiro-Wilk normality test) was performed on all the data shown. Accordingly, parametric two tailed unpaired student's t-test was applied on normally distributed data while non-parametric Mann-Whitney U test was applied on data which was not normally distributed to measure statistical significance. One way-ANOVA or Two way-ANOVA with Bonferroni Post-hoc test has been used for multiple comparisons.

Supplementary Material

Refer to Web version on PubMed Central for supplementary material.

Acknowledgements:

We thank Dr. Praveen Kumar of the Proteomics facility, University of Hyderabad for technical assistance in SPR experiments, and Aman Mishra for help in visualizing data. We thank the FACS and confocal microscopy core facilities of University of Hyderabad.

Funding: This work was supported by grants from Department of Science and Technology, Nano Mission, Government of India [DST No. SR/NM/NS-1040/2013(G)], and University Grants Commission, Government of India [UGC No. MRP-MAJOR-BIOT-2013-40689] to NK, and from the National Institutes of Health (AI129422 to AA and WH and AI137822 to WH). JE was supported by T32 EB023860.

References and Notes

1. Grohmann U, Mondanelli G, Belladonna ML, Orabona C, Pallotta MT, Iacono A, Puccetti P, Volpi C, Amino-acid sensing and degrading pathways in immune regulation. Cytokine Growth Factor Rev35, 37–45 (2017). [PubMed: 28545736]
2. Hotamisligil GS, Foundations of Immunometabolism and Implications for Metabolic Health and Disease. Immunity47, 406–420 (2017). [PubMed: 28930657]
3. Hotamisligil GS, Erbay E, Nutrient sensing and inflammation in metabolic diseases. Nat. Rev. Immunol8, 923–934 (2008). [PubMed: 19029988]
4. Saeed F, Nadeem M, Ahmed RS, Tahir Nadeem M, Arshad MS, Ullah A, Studying the impact of nutritional immunology underlying the modulation of immune responses by nutritional compounds – a review. Food Agric. Immunol27, 205–229 (2016).
5. Martí A, Marcos A, a Martínez J, Obesity and immune function relationships. Obes. Rev2, 131–140 (2001). [PubMed: 12119664]
6. Gallinetti J, Harputlugil E, Mitchell JR, Amino acid sensing in dietary-restriction-mediated longevity: roles of signal-transducing kinases GCN2 and TOR, Biochem. J449, 1–10 (2013). [PubMed: 23216249]
7. Goldberg EL, Romero-Aleshire MJ, Renkema KR, Ventevogel MS, Chew WM, Uhrlaub JL, Smithey MJ, Limesand KH, Sempowski GD, Brooks HL, Nikolich-Žugich J, Lifespan-extending caloric restriction or mTOR inhibition impair adaptive immunity of old mice by distinct mechanisms, Aging Cell14, 130–138 (2015). [PubMed: 25424641]
8. Battu S, Minhas G, Mishra A, Khan N, Amino acid sensing via general control nonderepressible-2 kinase and immunological programming, Front. Immunol8 (2017), 10.3389/fimmu.2017.01719.
9. Chandra RK, Antibody formation in first and second generation offspring of nutritionally deprived rats, Science (80-.). (1975), 10.1126/science.1179211.
10. Christadoss P, Talal N, Lindstrom J, Fernandes G, Suppression of cellular and humoral immunity to T-dependent antigens by calorie restriction, Cell. Immunol (1984), 10.1016/0008-8749(84)90046–7.
11. Gardner EM, Caloric restriction decreases survival of aged mice in response to primary influenza infection, Journals Gerontol. - Ser. A Biol. Sci. Med. Sci (2005), 10.1093/gerona/60.6.688.
12. Goldberg EL, Romero-Aleshire MJ, Renkema KR, Ventevogel MS, Chew WM, Uhrlaub JL, Smithey MJ, Limesand KH, Sempowski GD, Brooks HL, Nikolich-Žugich J, Lifespan-extending caloric restriction or mTOR inhibition impair adaptive immunity of old mice by distinct mechanisms, Aging Cell (2015), 10.1111/acel.12280.
13. Clinthorne JF, Gardner EM, Adams DJ, Fenton JI, Ritz BW, Short-Term Re-Feeding of Previously Energy-Restricted C57BL/6 Male Mice Restores Body Weight and Body Fat and Attenuates the Decline in Natural Killer Cell Function after Primary Influenza Infection, J. Nutr (2010), 10.3945/jn.110.122408.
14. Fernandes G, Tomar V, Venkatraman MN,JT, Potential of Diet Therapy on Murine AIDS, J. Nutr (2018), 10.1093/jn/122.suppl_3.716.
15. Messaoudi I, Warner J, Fischer M, Park B, Hill B, Mattison J, Lane MA, Roth GS, Ingram DK, Picker LJ, Douek DC, Mori M, Nikolich-Zugich J, Delay of T cell senescence by caloric restriction in aged long-lived nonhuman primates, Proc. Natl. Acad. Sci103, 19448–19453 (2006). [PubMed: 17159149]
16. Nikolich-Žugich J, Messaoudi I, Mice and flies and monkeys too: Caloric restriction rejuvenates the aging immune system of non-human primates, Exp. Gerontol40, 884–893 (2005). [PubMed: 16087306]
17. Yang H, Youm Y-H, Dixit VD, Inhibition of Thymic Adipogenesis by Caloric Restriction Is Coupled with Reduction in Age-Related Thymic Involution, J. Immunol183, 3040–3052 (2009). [PubMed: 19648267]

18. Yang H, Youm Y-H, Sun Y, Rim J-S, Galban CJ, Vandanmagsar B, Dixit VD, Axin expression in thymic stromal cells contributes to an age-related increase in thymic adiposity and is associated with reduced thymopoiesis independently of ghrelin signaling, J. Leukoc. Biol85, 928–938 (2009). [PubMed: 19299626]

19. Grossmann A, Maggio-Price L, Jinneman JC, Wolf NS, Rabinovitch PS, The effect of long-term caloric restriction on function of T-cell subsets in old mice, Cell. Immunol131, 191–204 (1990). [PubMed: 2121372]

20. Spaulding CC, Walford RL, Effros RB, in Mechanisms of Ageing and Development, (1997), vol. 93, pp. 25–33. [PubMed: 9089568]

21. Mejia P, Treviño-Villarreal JH, Hine C, Harputlugil E, Lang S, Calay E, Rogers R, Wirth D, Duraisingh MT, Mitchell JR, Dietary restriction protects against experimental cerebral malaria via leptin modulation and T-cell mTORC1 suppression, Nat. Commun6 (2015), 10.1038/ncomms7050.

22. McGettrick AF, O'Neill LAJ, How metabolism generates signals during innate immunity and inflammation, J. Biol. Chem288, 22893–22898 (2013). [PubMed: 23798679]

23. Murray PJ, Amino acid auxotrophy as a system of immunological control nodes, Nat. Immunol (2016), 10.1038/ni.3323.

24. González A, Hall MN, Nutrient sensing and TOR signaling in yeast and mammals, EMBO J36, 397–408 (2017). [PubMed: 28096180]

25. Battu S, Afroz S, Giddaluru J, Naz S, Huang W, Khumukcham SS, Khan RA, Bhat S, Qureshi IA, Manavathi B, Khan AA, August A, Hasnain SE, Khan N, Amino acid starvation sensing dampens IL-1β production by activating riboclustering and autophagy, PLOS Biol16, e2005317 (2018). [PubMed: 29621237]

26. Qin P, Arabacilar P, Bernard RE, Bao W, Olzinski AR, Guo Y, Lal H, Eisennagel SH, Platchek MC, Xie W, del Rosario J, Nayal M, Lu Q, Roethke T, Schnackenberg CG, Wright F, Quaile MP, Halsey WS, Hughes AM, Sathe GM, Livi GP, Kirkpatrick RB, Qu XA, Rajpal DK, Savitski MF, Bantscheff M, Joberty G, Bergamini G, Force TL, Gatto GJ, Hu E, Willette RN, Activation of the amino acid response pathway blunts the effects of cardiac stress, J. Am. Heart Assoc6 (2017), 10.1161/JAHA.116.004453.

27. Keller TL, Zocco D, Sundrud MS, Hendrick M, Edenius M, Yum J, Kim YJ, Lee HK, Cortese JF, Wirth DF, Dignam JD, Rao A, Yeo CY, Mazitschek R, Whitman M, Halofuginone and other febrifugine derivatives inhibit prolyl-tRNA synthetase, Nat Chem Biol8, 311–317 (2012). [PubMed: 22327401]

28. Guo F, Cavener DR, The GCN2 eIF2α Kinase Regulates Fatty-Acid Homeostasis in the Liver during Deprivation of an Essential Amino Acid, Cell Metab5, 103–114 (2007). [PubMed: 17276353]

29. Huebner KD, Jassal DS, Halevy O, Pines M, Anderson JE, Functional resolution of fibrosis in mdx mouse dystrophic heart and skeletal muscle by halofuginone, Am. J. Physiol. Circ. Physiol294, H1550–H1561 (2008).

30. Turgeman T, Hagai Y, Huebner K, Jassal DS, Anderson JE, Genin O, Nagler A, Halevy O, Pines M, Prevention of muscle fibrosis and improvement in muscle performance in the mdx mouse by halofuginone, Neuromuscul. Disord18, 857–868 (2008). [PubMed: 18672370]

31. Elkin M, Ariel I, Miao HQ, Nagler A, Pines M, De-Groot N, Hochberg A, Vlodavsky I, Inhibition of bladder carcinoma angiogenesis, stromal support, and tumor growth by halofuginone, Cancer Res59, 4111–4118 (1999). [PubMed: 10463616]

32. Pines M, Halofuginone for fibrosis, regeneration and cancer in the gastrointestinal tract, World J. Gastroenterol20, 14778–14786 (2014). [PubMed: 25356039]

33. Ravindran R, Loebbermann J, Nakaya HIHI, Khan N, Ma H, Gama L, Machiah DKDK, Lawson B, Hakimpour P, Wang YYC, Li S, Sharma P, Kaufman RJRJ, Martinez J, Pulendran B, The amino acid sensor GCN2 controls gut inflammation by inhibiting inflammasome activation, Nature531, 1–17 (2016).

34. Sundrud MS, Koralov SB, Feuerer M, Calado DP, Kozhaya AE, Rhule-Smith A, Lefebvre RE, Unutmaz D, Mazitschek R, Waldner H, Whitman M, Keller T, Rao A, Halofuginone inhibits TH17

cell differentiation by activating the amino acid starvation response, Science (80-.).324, 1334–1338 (2009).

35. Querec TD, Akondy RS, Lee EK, Cao W, Nakaya HI, Teuwen D, Pirani A, Gernert K, Deng J, Marzolf B, Kennedy K, Wu H, Bennouna S, Oluoch H, Miller J, Vencio RZ, Mulligan M, Aderem A, Ahmed R, Pulendran B, Systems biology approach predicts immunogenicity of the yellow fever vaccine in humans., Nat. Immunol10, 116–25 (2009). [PubMed: 19029902]
36. Ravindran R, Khan N, Nakaya HI, Li S, Loebbermann J, Maddur MS, Park Y, Jones DP, Chappert P, Davoust J, Weiss DS, Virgin HW, Ron D, Pulendran B, Vaccine activation of the nutrient sensor GCN2 in dendritic cells enhances antigen presentation., Science343, 313–7 (2014). [PubMed: 24310610]
37. Van de Velde LA, Guo XZJ, Barbaric L, Smith AM, Oguin TH, Thomas PG, Murray PJ, Stress Kinase GCN2 Controls the Proliferative Fitness and Trafficking of Cytotoxic T Cells Independent of Environmental Amino Acid Sensing, Cell Rep17, 2247–2258 (2016). [PubMed: 27880901]
38. Low JGH, Ooi EE, Vasudevan SG, Current status of dengue therapeutics research and development, J. Infect. Dis (2017), 10.1093/infdis/jiw423.
39. Guzman MG, Hermida L, Bernardo L, Ramirez R, Guillén G, Domain III of the envelope protein as a dengue vaccine target, Expert Rev. Vaccines (2010), 10.1586/erv.09.139.
40. Ye J, Kumanova M, Hart LS, Sloane K, Zhang H, De Panis DN, Bobrovnikova-Marjon E, Diehl JA, Ron D, Koumenis C, The GCN2-ATF4 pathway is critical for tumour cell survival and proliferation in response to nutrient deprivation, EMBO J29, 2082–2096 (2010). [PubMed: 20473272]
41. Harty JT, Badovinac VP, Shaping and reshaping CD8+ T-cell memory, Nat. Rev. Immunol (2008), 10.1038/nri2251.
42. Homann D, Teyton L, Oldstone MBA, Differential regulation of antiviral T-cell immunity results in stable CD8+ but declining CD4+ T-cell memory, Nat. Med (2001), 10.1038/90950.
43. Kasturi SP, Skountzou I, Albrecht RA, Koutsonanos D, Hua T, Nakaya HI, Ravindran R, Stewart S, Alam M, Kwissa M, Villinger F, Murthy N, Steel J, Jacob J, Hogan RJ, García-Sastre A, Compans R, Pulendran B, Programming the magnitude and persistence of antibody responses with innate immunity., Nature470, 543–7 (2011). [PubMed: 21350488]
44. Haring JS, Badovinac VP, Harty JT, Inflaming the CD8+ T Cell Response, Immunity (2006), 10.1016/j.immuni.2006.07.001.
45. Leo O, Cunningham A, Stern PL, Vaccine immunology, Perspect. Vaccinol1, 25–59 (2011).
46. Fazilleau N, Chakarov S, Monocyte-derived dendritic cells identified as booster of T follicular helper cell differentiation, EMBO Mol. Med6, 590–603 (2014). [PubMed: 24737871]
47. Hangartner L, Zinkernagel RM, Hengartner H, Antiviral antibody responses: The two extremes of a wide spectrum, Nat. Rev. Immunol6, 231–243 (2006). [PubMed: 16498452]
48. Chaimowitz NS, Martin RK, Cichy J, Gibb DR, Patil P, Kang D-J, Farnsworth J, Butcher EC, McCright B, Conrad DH, A Disintegrin and Metalloproteinase 10 Regulates Antibody Production and Maintenance of Lymphoid Architecture, J. Immunol187, 5114–5122 (2011). [PubMed: 21998451]
49. McHeyzer-Williams LJ, McHeyzer-Williams MG, ANTIGEN-SPECIFIC MEMORY B CELL DEVELOPMENT, Annu. Rev. Immunol23, 487–513 (2005). [PubMed: 15771579]
50. Choi SC, Titov AA, Abboud G, Seay HR, Brusko TM, Roopenian DC, Salek-Ardakani S, Morel L, Inhibition of glucose metabolism selectively targets autoreactive follicular helper T cells, Nat. Commun (2018), 10.1038/s41467-018-06686-0.
51. Pratama A, Vinuesa CG, Control of TFH cell numbers: Why and how? Immunol. Cell Biol (2014), 10.1038/icb.2013.69.
52. Laidlaw BJ, Lu Y, Amezquita RA, Weinstein JS, Vander Heiden JA, Gupta NT, Kleinstein SH, Kaech SM, Craft J, Interleukin-10 from CD4+ follicular regulatory T cells promotes the germinal center response, Sci. Immunol2 (2017), 10.1126/sciimmunol.aan4767.
53. Guthmiller JJ, Graham AC, Zander RA, Pope RL, Butler NS, Cutting Edge: IL-10 Is Essential for the Generation of Germinal Center B Cell Responses and Anti-Plasmodium Humoral Immunity., J. Immunol198, 617–622 (2017). [PubMed: 27940658]

54. Lanzavecchia A, Dissecting human antibody responses: useful, basic and surprising findings, EMBO Mol. Med e8879 (2018). [PubMed: 29363490]
55. Alabyev B, Manser T, Bcl-2 rescues the germinal center response but does not alter the V gene somatic hypermutation spectrum in MSH2-deficient mice., J. Immunol169, 3819–24 (2002). [PubMed: 12244177]
56. Hikida M, Casola S, Takahashi N, Kaji T, Takemori T, Rajewsky K, Kurosaki T, PLC-gamma2 is essential for formation and maintenance of memory B cells., J. Exp. Med206, 681–9 (2009). [PubMed: 19273623]
57. Takemori T, Kaji T, Takahashi Y, Shimoda M, Rajewsky K, Generation of memory B cells inside and outside germinal centers, Eur. J. Immunol44, 1258–1264 (2014). [PubMed: 24610726]
58. Ding Y, Li J, Wu Q, Yang P, Luo B, Xie S, Druey KM, Zajac AJ, Hsu H-C, Mountz JD, IL-17RA Is Essential for Optimal Localization of Follicular Th Cells in the Germinal Center Light Zone To Promote Autoantibody-Producing B Cells, J. Immunol191, 1614–1624 (2013). [PubMed: 23858031]
59. Recaldin T, Fear DJ, Transcription factors regulating B cell fate in the germinal centre, Clin. Exp. Immunol183, 65–75 (2016). [PubMed: 26352785]
60. Kirstetter P, Thomas M, Dierich A, Kastner P, Chan S, Ikaros is critical for B cell differentiation and function, Eur. J. Immunol32, 720–730 (2002). [PubMed: 11870616]
61. Mcgaha TL, Metz R, Prendergast GC, Mellor AL, Amino acid catabolism: a pivotal regulator of innate and adaptive immunity, Immunol. Rev249, 135–157 (2012). [PubMed: 22889220]
62. Lynch HE, Stewart SM, Kepler TB, Sempowski GD, Alam SM, Surface plasmon resonance measurements of plasma antibody avidity during primary and secondary responses to anthrax protective antigen, J. Immunol. Methods404, 1–12 (2014). [PubMed: 24316020]
63. Chen C, Zhai S, Zhang L, Chen J, Long X, Qin J, Li J, Huo R, Wang X, Uhrf1 regulates germinal center B cell expansion and affinity maturation to control viral infection, 1–15 (2018).
64. Deng X-M, Yan S-X, Wei W, IL-21 acts as a promising therapeutic target in systemic lupus erythematosus by regulating plasma cell differentiation, Cell. Mol. Immunol1258, 31–39 (2015).
65. Jaiswal S, Khanna N, Swaminathan S, High-level expression and one-step purification of recombinant dengue virus type 2 envelope domain III protein in Escherichia coli, Protein Expr. Purif33, 80–91 (2004). [PubMed: 14680965]
66. Afroz S, Giddaluru J, Vishwakarma S, Naz S, Khan AA, Khan N, A comprehensive gene expression meta-analysis identifies novel immune signatures in rheumatoid arthritis patients, Front. Immunol8 (2017), 10.3389/fimmu.2017.00074.
67. Afroz S, Medhi H, Maity S, Minhas G, Battu S, Giddaluru J, Kumar K, Paik P, Khan N, Mesoporous ZnO nanocapsules for the induction of enhanced antigen-specific immunological responces, Nanoscale9, 14641–14653 (2017). [PubMed: 28936523]
68. Vervaeke P, Alen M, Noppen S, Schols D, Oreste P, Liekens S, Sulfated Escherichia coli K5 Polysaccharide Derivatives Inhibit Dengue Virus Infection of Human Microvascular Endothelial Cells by Interacting with the Viral Envelope Protein E Domain III, PLoS One8 (2013), 10.1371/journal.pone.0074035.
69. Staats HF, Alam SM, Scearce RM, Kirwan SM, Zhang JX, Gwinn WM, Haynes BF, In vitro and in vivo characterization of anthrax anti-protective antigen and anti-lethal factor monoclonal antibodies after passive transfer in a mouse lethal toxin challenge model to define correlates of immunity, Infect. Immun75, 5443–5452 (2007). [PubMed: 17709410]
70. Medina F, Francisco Medina J, Colón C, Vergne E, Santiago G, L Muñoz-Jordán J, Dengue Virus: Isolation, Propagation, Quantification, and Storage, Curr. Protoc. Microbiol Chapter 15, Unit15D.2 (2012).
71. Leng CH, Liu SJ, Tsai JP, Li YS, Chen MY, Liu HH, Lien SP, Yueh A, Hsiao KN, Lai LW, Liu FC, Chong P, Chen HW, A novel dengue vaccine candidate that induces cross-neutralizing antibodies and memory immunity, Microbes Infect11, 288–295 (2009). [PubMed: 19114121]
72. Poggianella M, Campos JLS, Chan KR, Tan HC, Bestagno M, Ooi EE, Burrone OR, Dengue e protein domain iii-based dna immunisation induces strong antibody responses to all four viral serotypes, PLoS Negl. Trop. Dis9, 1–28 (2015).

73. Afroz S, Giddaluru J, Manzar Abbas M, Khan N, Transcriptome meta-analysis reveals a dysregulation in extra cellular matrix and cell junction associated gene signatures during Dengue virus infection, Nat. Publ. Gr, 1–12 (2016).

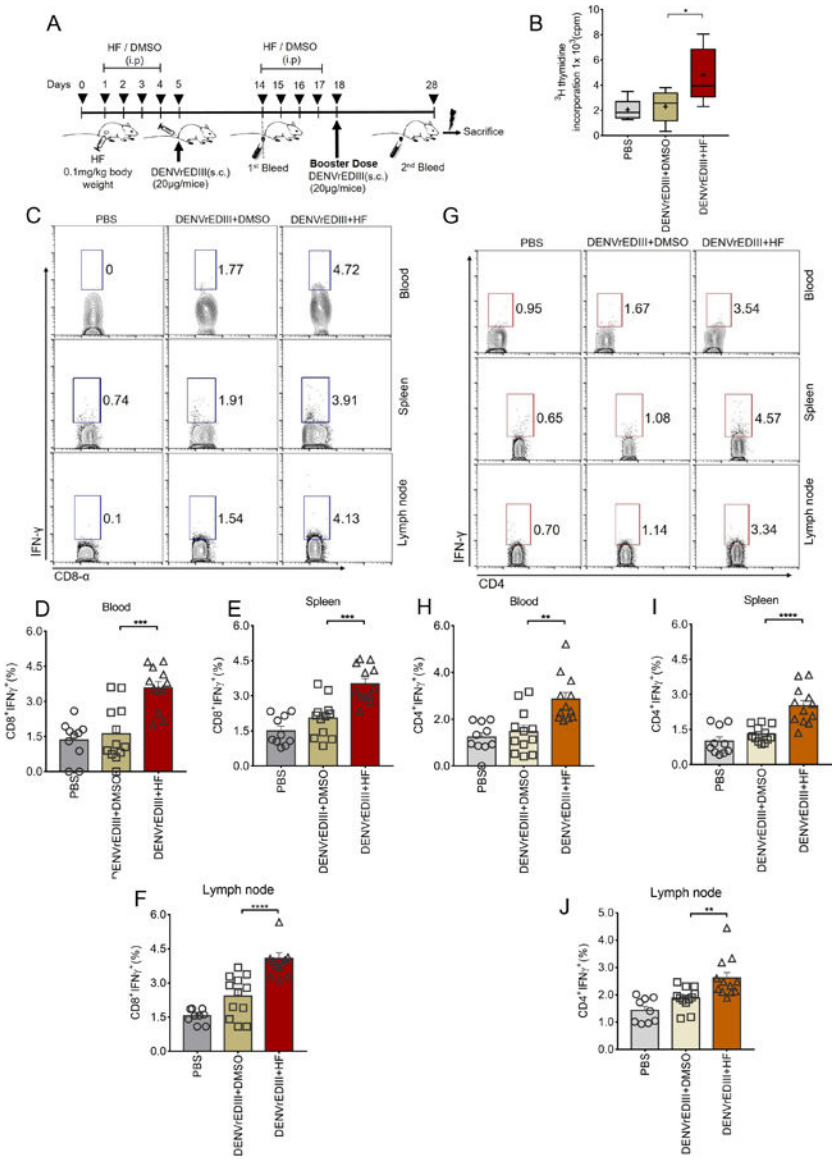

Fig. 1. HF enhances antigen-specific T-cell responses in-vivo.

(**A**) Experimental outline of HF or vehicle control DMSO treatment and DENV-2 envelope domain III (DENVrEDIII) protein immunization. (**B**) Proliferation analysis by ^{3}H thymidine incorporation in antigen specific T-cells from splenocytes of mice 28 days after immunization that were restimulated with DENVrEDIII protein. Data are means ± SEM of 12 mice per treatment group from 2 independent experiments.(**C** to **J**) Flow cytometry analysis of DENVrEDIII-specific CD8^{+}(C to F) and CD4^{+}(G to J) T-cell responses in blood (D and H), spleen (E and I) and lymph node (F and J) after treatment and immunization, as indicated. FACS plots (C and G) are representative of 2 independent experiments. Quantification of the percentage of IFN-γ producing T-cells (D to F, and H to J) are means ± SEM of 12 mice per treatment group from 2 experiments. *P<0.05, **P<0.01, ***P<0.001, ****P<0.0001 by two tailed unpaired student *t* test (B) and Mann-Whitney U test (D, E, F, H, I and J).

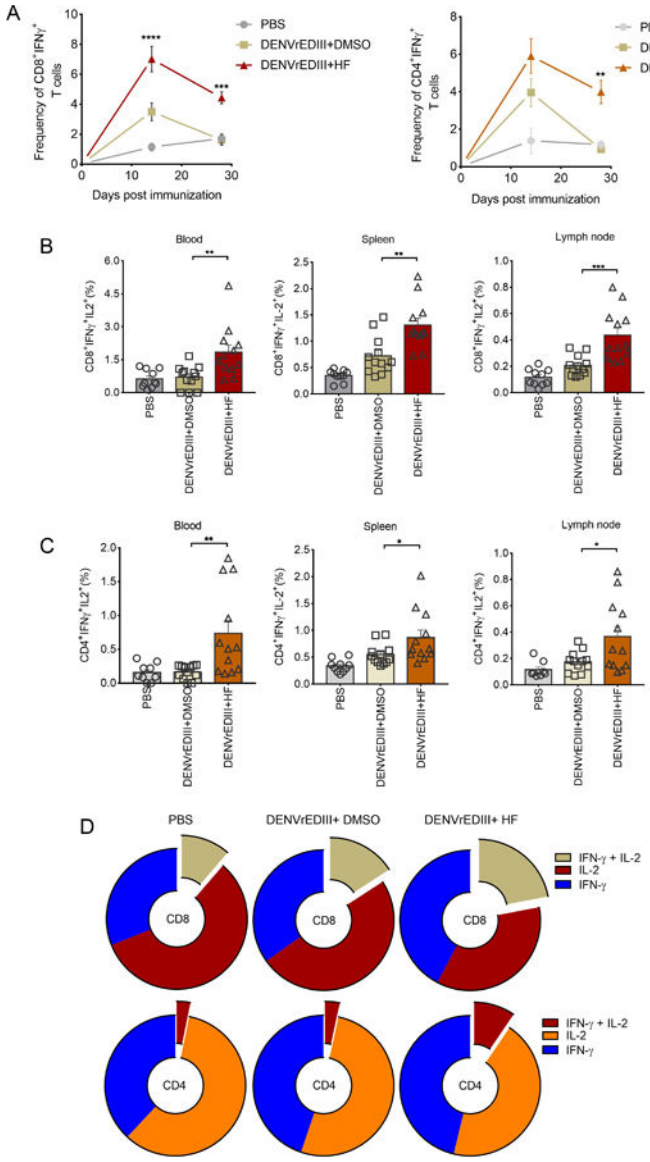

Fig. 2. HF increases the frequency of antigen-specific polyfunctional T-cells in mice.

(**A**) Flow cytometry analysis of antigen-specific $CD8^+IFN\text{-}\gamma^+$ and$CD4^+IFN\text{-}\gamma^+$ T-cell kinetics in PBMCs of mice treated with DMSO or HF and immunized with DENV-2 envelope domain III after 14 and 28 days. Data are means ± SEM of 12 mice/group from 2 independent experiments. **(B** to **D)** Flow cytometry analysis of DENVrEDIII-specific polyfunctional $CD8^+$ (B) and $CD4^+$(C) T-cells in blood, spleen and lymph node of immunized mice. The frequency of double cytokine (IFN-γ and IL-2) producing cells with means (bar) ± SEM (B and C) and pie charts of the frequency of all cytokine producing T-cells (D) are from 12 mice/group from 2 independent experiments.*P<0.05, **P<0.01, ***P<0.001, ****P<0.0001by 2-way ANOVA with Bonferroni post-hoc between DENVrEDIII+DMSO and DENVrEDIII+HF immunized groups(A), Mann-Whitney U test(B and C)

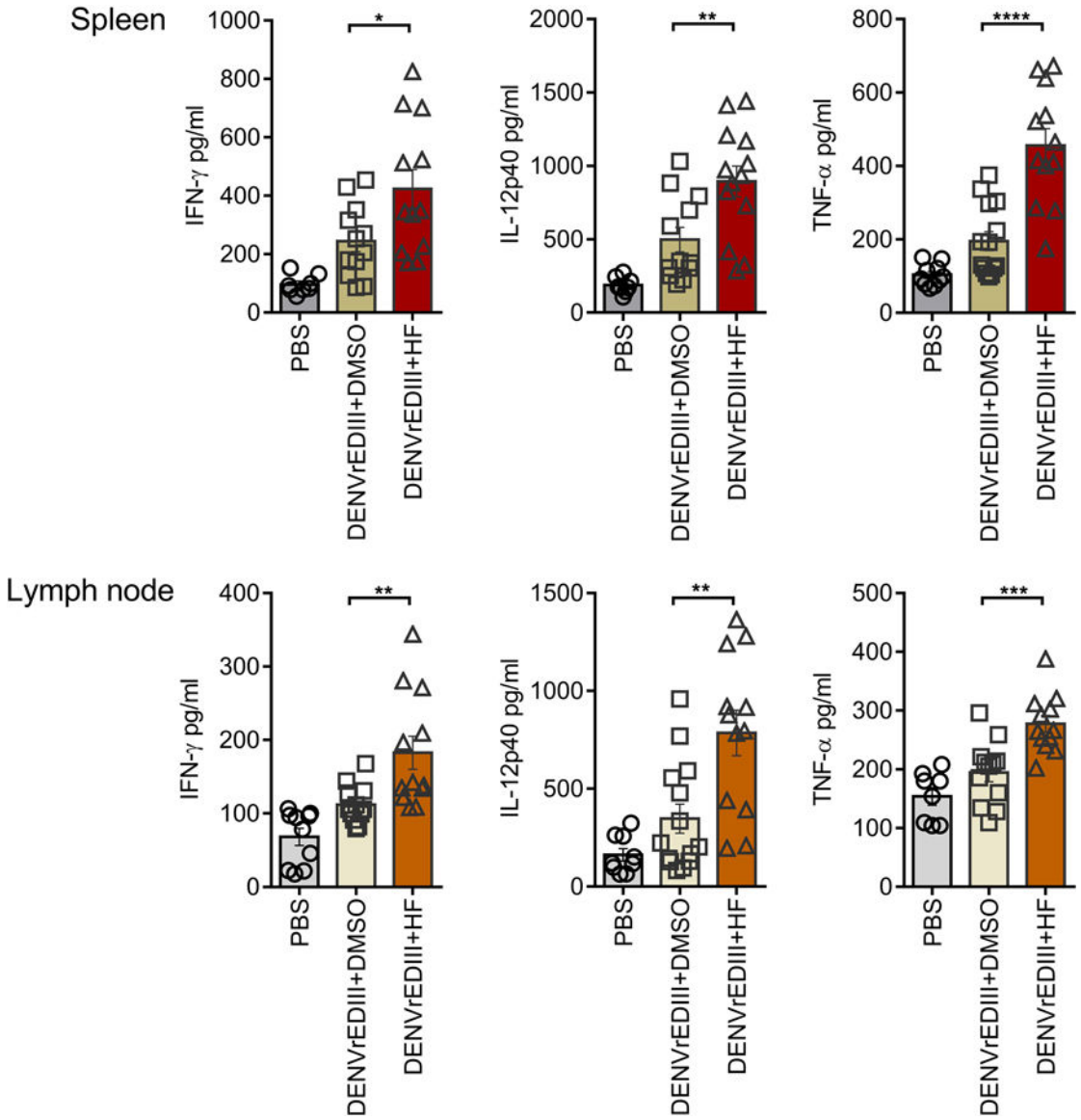

Fig. 3. HF enhances secretion of multiple cytokines after DENVrEDIII immunization.

ELISA analysis of the amounts of IFN-γ, IL-12p40 and TNF-α produced bysplenocytes and lymph node cells from immunized mice after re-stimulation in vitro with DENVrEDIII for 72hr. Spleen and lymph nodes were collected from mice at 28th day post-secondary immunization. Data are means ± SEM from 12 mice per treatment group from 2 independent experiments. *P<0.05, **P<0.01, ***P<0.001, ****P<0.0001 by two tailed unpaired student *t* test.

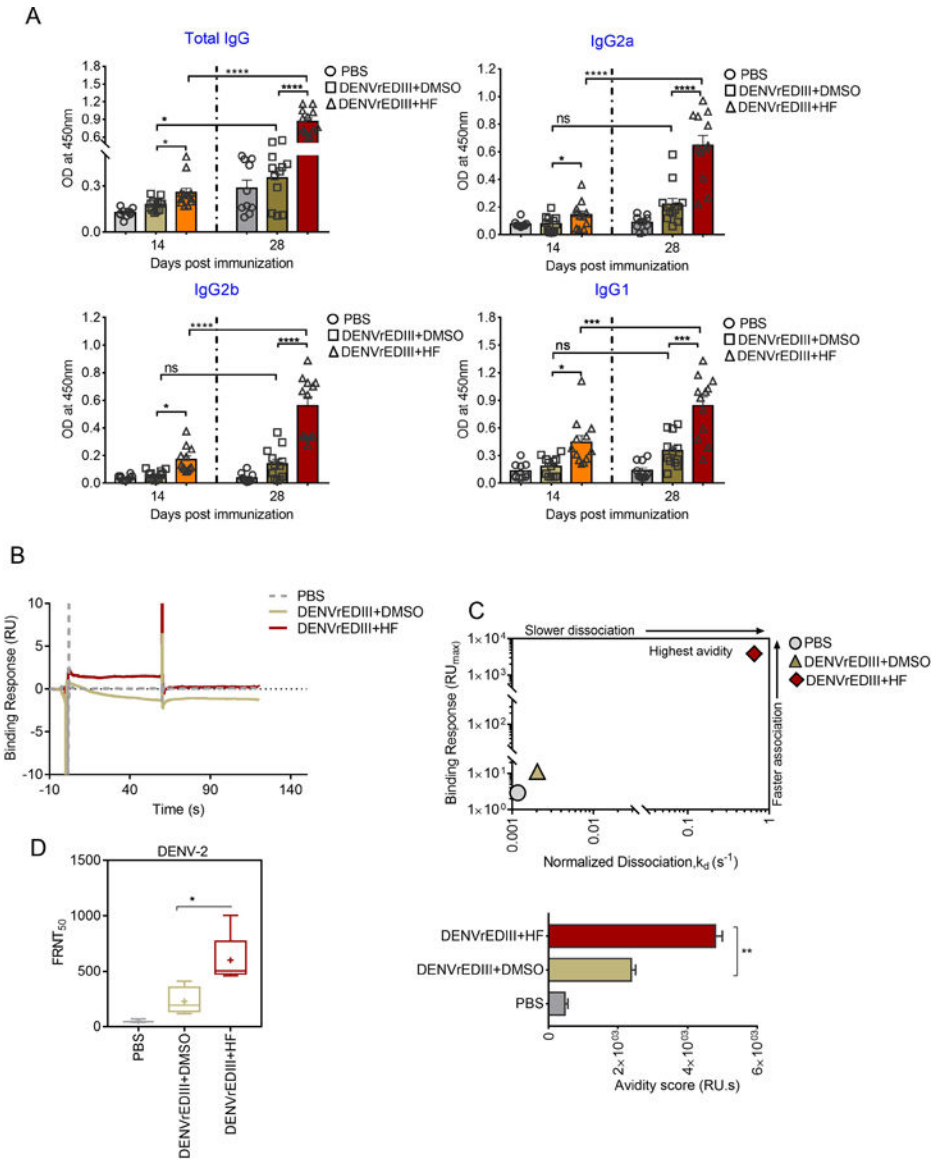

Fig. 4. HF mediated AAR activation augments of antibody responses against DENVrEDIII.

(A) ELISA analysis of DENVrEDIII specific total IgG, IgG2a, IgG2b, and IgG1 in the serum of mice14 days after primary immunization and 28 days after secondary immunization. Data are means ± SEM of 12 mice/group from 2 independent experiments. **(B** and **C)** BIAcore SPR analysis of DENVrEDIII protein binding by pooled serum samples from mice preconditioned with HF or DMSO 28 days after immunization. Sensogram trace of the DENVrEDIII-specific antibody binding affinity (B) and correlation of the Maximal Response Unit (RU_{max}) with the dissociation constant (C, upper) are representative of 2 independent experiments. Quantified avidity scores(C, lower) are means ± SEM from 2 independent experiments on pooled serum samples from 10 mice/group assayed in triplicate. **(D)** DENV-2 virus neutralization assay on serum samples collected from mice 28 days after immunization. The 50% focus reduction neutralization titre ($FRNT_{50}$) data are means ± SEM of 10 mice from 2 independent experiments assayed in triplicate.*P<0.05, **P<0.01,

***P<0.001, ****P<0.0001, by one-way ANOVA with Bonferroni post-hoc test (A), two tailed unpaired student *t* test(C) and Mann-Whitney U test (D).

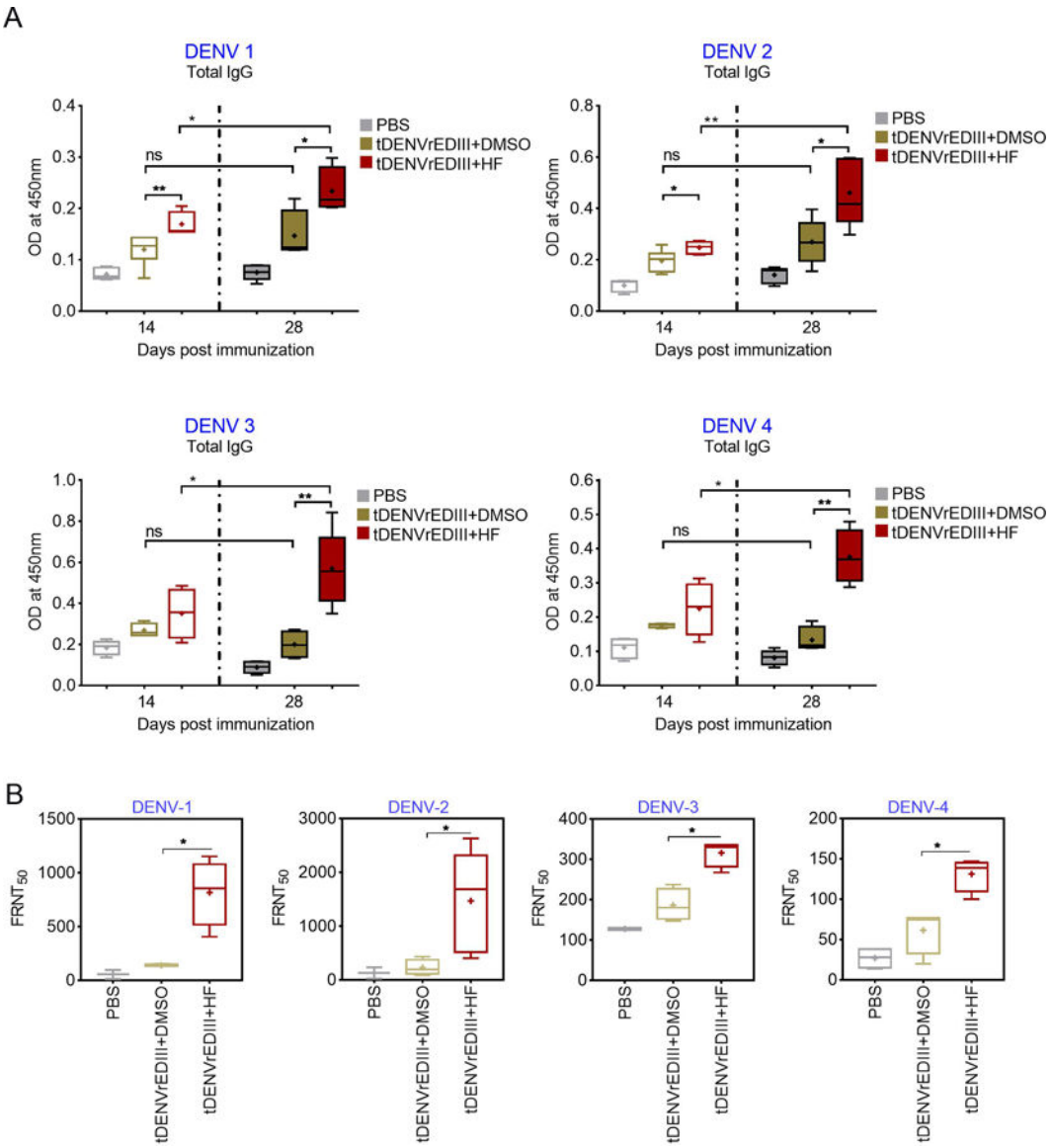

Fig. 5. HF enhances the antibody response to a tetravalent DEN vaccine.

(A)ELISA of total IgG specific for all four DENV serotypes in the serum of mice immunized with a tetravalent combination of DENVrEDIII protein 14 days after primary immunization and 28 days after secondary immunization. Data are means ± SEMof10 mice/ group from 2 independent experiments. **(B)**DENV serotype neutralization assay on serum from tDENVrEDIII immunized mice. The 50% focus reduction neutralization titre ($FRNT_{50}$) data are means ± SEM of 10 mice from 2 independent experiments. *P<0.05, **P<0.01 by one-way ANOVA with Bonferroni post-hoc test (A) and Mann-Whitney U test (B).

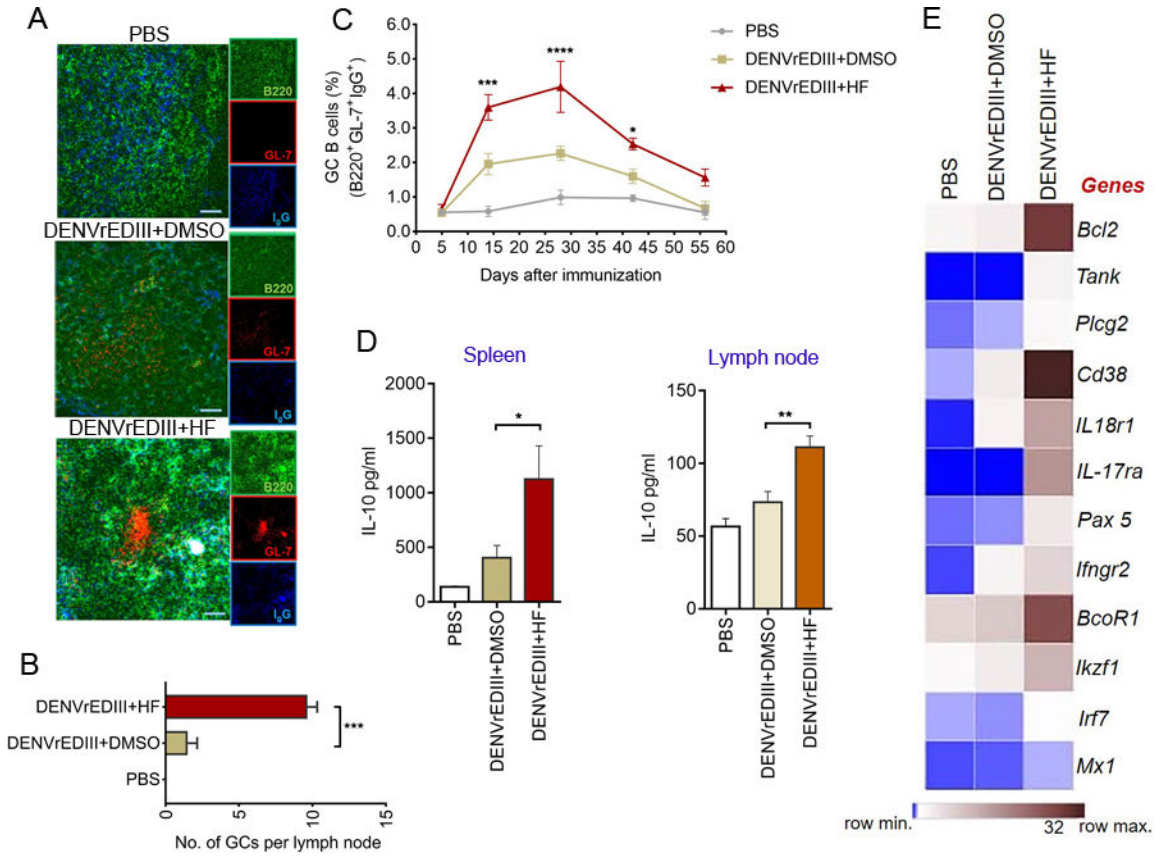

Fig. 6. HF pre-treatment in DENVrEDIII immunized mice enhances GC formation.

(A and **B)** Confocal microscopy imaging of the GL-7^{+}(red), B220^{+}(green) IgG^{+}(blue) GC B-cells in lymph node sections from mice treated with HF or DMSO and immunized with DENVrEDIII protein. Images (A) are representative of 2 independent experiments. Quantified data (B) are means ± SEM of 8 mice/condition from all experiments. **(C)** Flow cytometry analysis of lymph node GC-B cells frequency in DENVrEDIII immunized mice at the indicated time-points. Data are means ± SEM of 8 mice per group at each time-point from 2 independent experiments.**(D)** ELISA analysis of IL-10 production by splenocytes and lymph node cells from mice 28 days after secondary immunization that were restimulated with DENVrEDIII. Data are means ± SEM of 10 mice/group from 2 independent experiments. **(E)** qRT-PCR analysis of the indicated gene expression in lymph node cells restimulated with DENVrEDIII for 24hr. Heatmap of statistically significant changes are from the analysis of 10 biological replicates from 2 independent experiments. *P<0.05, **P< 0.01, ***P<0.001, ****P<0.0001by two tailed unpaired student *t* test (B and D) and 2-way ANOVA with Bonferroni Post-hoc test (C).